

OPTIMAL FUZZY DESIGN OF CHUA'S CIRCUIT SYSTEM

CHIH-CHING HUNG¹, TIM CHEN^{2,*}, ABU ABI ASTOLFI³, SINGIRES RIO RAO^{4,5}
HONG-TSU YOUNG¹, CHENCHENG WUTIM⁶ AND CYJ CHEN^{7,8,*}

¹Department of Mechanical Engineering
National Taiwan University
No. 1, Sec. 4, Roosevelt Road, Taipei 10617, Taiwan

²AI Lab, Faculty of Information Technology
Ton Duc Thang University
19 Nguyen Huu Tho Street, Tan Phong Ward, District 7, Ho Chi Minh City 700000, Vietnam

*Corresponding author: timchen@tdtu.edu.vn

³Department of Electrical and Electronic Engineering
University of Bath
Bath, BA2 7AY U.K.

⁴Department of Mechanical and Aerospace Engineering

⁵High Performance Computing Research Center
University of Minnesota
89 Church St. S.E., Minneapolis 55455, USA

⁶Department of Mechanical Engineering
Debre Tabor University
P.O.BOX 272, Debre Tabor, Ethiopia

⁷NAAM Research Group
King Abdulaziz University
Al Jamiaa District 80200, Jeddah 21589, Saudi Arabia

⁸Department of Artificial Intelligence
University of Maryland
Maryland 20742, USA

*Corresponding author: jc343965@gmail.com; cyjchen@umd.edu

Received January 2019; revised May 2019

ABSTRACT. *This paper addresses the robust controller design problem for a class of fuzzy-neural systems that are robust against both the plant parameter perturbations and controller gain variations. More specifically, the purpose is to synthesize a piecewise Static Output Feedback (SOF) controller guaranteeing the stability of the resulting closed-loop fuzzy-neural dynamic system. Based on piecewise quadratic Lyapunov functions and the relaxed method with Neural Network Differential Inclusion (NNDI), the intelligent approach can be stabilized by regulating appropriately the parameters of dither and this robust controller gains can be obtained by solving a set of Linear Matrix Inequalities (LMIs). The superiority of proposed method is verified through numerical examples. Because the design of efficient and high-performance control systems is of fundamental interest to engineers, systematic methodologies are to be used for the combined intelligent and active control system synthesis in many applications.*

Keywords: Intelligent information, System control, Artificial intelligence

1. Introduction. Chaotic behavior is abundant both in nature and in man-made devices and has been extensively demonstrated in the last few years; see, for example, [1-3] and the references therein. Chaos is an irregular, seemingly random, dynamic behavior of a deterministic system displaying extreme sensitivity to initial conditions [4]. Moreover, chaos is occasionally desirable, but usually not expected since it can degrade performance and limit the operating range of many physical devices. Hence, the ability to control chaos is of much practical importance [1,5-7]. After the pioneering work of Ott, Grebogi and Yorke (OGY) [8], controlling chaos has become a challenging topic in the field of nonlinear dynamics [9].

It has long been known that the injection of a high frequency signal, known as a dither, into a nonlinear system, just ahead of the nonlinearity may improve its performance. Better performance is viewed as less distortion in the system output, augmented stability, quenching of limit cycles and jump phenomena [10]. A rigorous analysis of stability in a general nonlinear system with a dither control was given in [11]. It was shown that the trajectory of a dithered system can be predicted rigorously by establishing that of its corresponding mathematical model – the relaxed system (as defined later), provided the dither has a high enough frequency.

In brief, if a controller cannot stabilize the chaotic system, a dither of an auxiliary is injected into the chaotic system and then the chaotic system is stabilized asymptotically by regulating the dither's parameters. Moreover, system reliability analysis of modified support vector machines with particle swarm optimization is proposed for the improvement of the control system [18]. A increasing number of intelligent tools are used to analyze and design the controlled systems [19-22]. In order to catch up with the previous techniques, the purpose of this paper is to propose a novel approach to control chaos. The performance of chaotic systems is the sources of the instability and the criterion of the controlled system can be guaranteed by the proposed methodology in this paper. Section 2 is to consider a chaotic system with dithers and the parameters of dither are regulated such that the relaxed system is asymptotically stable. Section 3 is an example which demonstrated the relaxed system and dithered chaotic system have been controlled with the methodology. Section 4 shows the conclusions for the proposed design methodology.

2. System Description. Consider the chaotic system depicted by the following equation:

$$\dot{x}(t) = F(x, t), \quad (1)$$

where $x(t)$ is the state vector and F is a vector-valued function which satisfies those assumptions of general continuity and boundedness given in [11].

In order to eliminate the chaotic motion, a dither $d(t)$, with a finite number N of switchings, is injected into the chaotic system (1). Thus, the dithered chaotic system is described as

$$\dot{x}(t) = F(x, t, d). \quad (2)$$

The algorithm for constructing the dither signal is given as follows: The time interval $[0, T]$ is divided into an arbitrary number N of equal subintervals. The beginning of the first interval, the end of the first interval, the end of the second interval and the end of the N th interval are denoted by t_0, t_1, t_2 and t_N , respectively. Dividing every interval $[t_k, t_{k+1}]$ for $k = 0, 1, 2, \dots, N - 1$ into n subintervals, the length of the j th subinterval will be $\alpha_j(t_k)[t_{k+1} - t_k]$ for $j = 1, 2, \dots, n$ and the control $\beta_j(t_k)$ is applied at the j th subinterval. Hence the repetition frequency, shape and amplitude of dither can be determined by regulating the parameters $N, \alpha_j(t_k)$ and $\beta_j(t_k)$. In order to illustrate the algorithm, an example of constructing a periodic dither is given in the following figure.

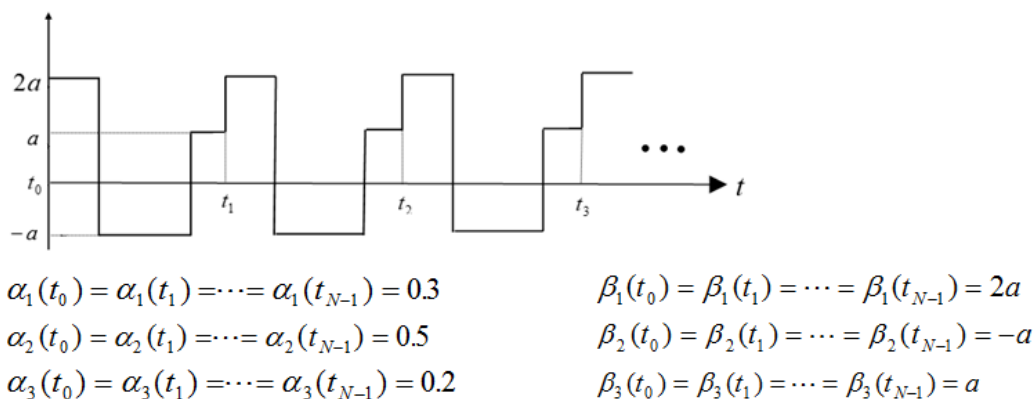


FIGURE 1. A periodic dither signal

From Figure 1 discussed above, we can infer that if the dither has a sufficiently large frequency and a proper membership function is chosen in fuzzy relaxed system.

The corresponding relaxed model of the dithered chaotic system (2) is defined as [11]:

$$\dot{x}_r(t) = \sum_{j=1}^n \alpha_j(t) F(x_r, t, \beta_j), \quad (3)$$

$$0 \leq \alpha_j(t) \leq 1, \quad \sum_{j=1}^n \alpha_j(t) = 1. \quad (4)$$

2.1. The trajectory by dithered chaotic system. It was shown in [12] that the absolutely continuous curve $x_r(t)$ satisfying Equation (3) is the uniform limit of curves $x_N(t)$, $N = 1, 2, \dots$, satisfying Equation (2). That is to say, as the frequency of dither goes to infinity, the trajectory described by the dithered chaotic system (2) will approach that of the relaxed system (3). Hence, the relaxed system may be viewed as the mathematical model of the chaotic system with a dither of high enough frequency. If the relaxed system is asymptotically stable and the number N of switchings in $d(t)$ is chosen to be sufficiently large, then the dithered chaotic system is approximated by its corresponding mathematical model – the relaxed system and the approximation improves as N increases. Consequently, the behavior described by the dithered chaotic system and the behavior of the relaxed system would be made as close as desired, and then the chaotic motion is converted into a steady state.

2.2. Periodic dither signal. In real systems, the dither is generally chosen to be a periodic signal and then the parameters $\alpha_m(t)$ and $\beta_m(t)$ are independent of time. Hence, a periodic dither signal is considered in the remainder of this study [13-17].

IF $x_{R1}(t)$ is $M_{Ri1}(\alpha_m, \beta_m)$ and ... and $x_{Rk}(t)$ is $M_{Rik}(\alpha_m, \beta_m)$

$$\text{THEN } u_R(t) = -K_i \hat{x}_R(t), \quad i = 1, 2, \dots, r. \quad (5)$$

Observer Rule i :

IF $x_{R1}(t)$ is $M_{Ri1}(\alpha_m, \beta_m)$ and ... and $x_{Rk}(t)$ is $M_{Rik}(\alpha_m, \beta_m)$

$$\text{THEN } \dot{\hat{x}}_R(t) = A_i(\alpha_m, \beta_m) \hat{x}_R(t) + B_i(\alpha_m, \beta_m) u_R(t) + L_i (y_R(t) - \hat{y}_R(t)), \quad (6)$$

$$\text{where } y_R(t) = D_i(\alpha_m, \beta_m) x_R(t), \quad \hat{y}_R(t) = D_i(\alpha_m, \beta_m) \hat{x}_R(t) \text{ and } i = 1, 2, \dots, r. \quad (7)$$

Thus, the overall machine learning fuzzy controller and machine learning fuzzy observer can be written as:

$$u_R(t) = -\frac{\sum_{i=1}^r w_i(x_R(t), \alpha_m, \beta_m) K_i \hat{x}_R(t)}{\sum_{i=1}^r w_i(x_R(t), \alpha_m, \beta_m)}, \tag{8}$$

$$\dot{\hat{x}}_R(t) = \frac{\sum_{i=1}^r w_i(x_R(t), \alpha_m, \beta_m) \{A_i(\alpha_m, \beta_m) \hat{x}_R(t) + B_i(\alpha_m, \beta_m) u_R(t) + L_i (y_R(t) - \hat{y}_R(t))\}}{\sum_{i=1}^r w_i(x_R(t), \alpha_m, \beta_m)}, \tag{9}$$

where

$$\hat{y}_R(t) = \frac{\sum_{i=1}^r w_i(x_R(t), \alpha_m, \beta_m) D_i(\alpha_m, \beta_m) \hat{x}_R(t)}{\sum_{i=1}^r w_i(x_R(t), \alpha_m, \beta_m)}. \tag{10}$$

That means the control force could be regulated by the frequency of injected dither. Therefore, we get

$$= \frac{\sum_{i=1}^r \sum_{j=1}^r w_i(x_R(t), \alpha_m, \beta_m) w_j(x_R(t), \alpha_m, \beta_m) \{ (A_i(\alpha_m, \beta_m) x_R(t) - B_i(\alpha_m, \beta_m) K_j) \hat{x}_R(t) + L_i D_j(\alpha_m, \beta_m) (x_R(t) - \hat{x}_R(t)) \}}{\sum_{i=1}^r \sum_{j=1}^r w_i(x_R(t), \alpha_m, \beta_m) w_j(x_R(t), \alpha_m, \beta_m)}. \tag{11}$$

The augmented systems can be derived by the following equation:

$$\dot{x}_{Ra}(t) = \frac{\sum_{i=1}^r \sum_{j=1}^r w_i(x_R(t), \alpha_m, \beta_m) w_j(x_R(t), \alpha_m, \beta_m) \tilde{A}_{ij}(\alpha_m, \beta_m) x_{Ra}(t)}{\sum_{i=1}^r \sum_{j=1}^r w_i(x_R(t), \alpha_m, \beta_m) w_j(x_R(t), \alpha_m, \beta_m)}, \tag{12}$$

where $x_{Ra}(t) = \begin{bmatrix} x_R(t) \\ \tilde{x}_R(t) \end{bmatrix}$, $\tilde{x}_R(t) = x_R(t) - \hat{x}_R(t)$ and

$$\tilde{A}_{ij}(\alpha_m, \beta_m) = \begin{bmatrix} A_i(\alpha_m, \beta_m) - B_i(\alpha_m, \beta_m) K_j & B_i(\alpha_m, \beta_m) K_j \\ 0 & A_i(\alpha_m, \beta_m) - L_i D_j(\alpha_m, \beta_m) \end{bmatrix}. \tag{13}$$

The premise variables $x_R(t)$ depend on the state variables estimated by the machine learning fuzzy observer, which are unknown. The controller is

$$u_R(t) = -\frac{\sum_{i=1}^r w_i(\hat{x}_R(t), \alpha_m, \beta_m) K_i \hat{x}_R(t)}{\sum_{i=1}^r w_i(\hat{x}_R(t), \alpha_m, \beta_m)}. \tag{14}$$

Moreover, a machine learning fuzzy observer is

$$\dot{\hat{x}}_R(t) = \frac{\sum_{i=1}^r w_i(\hat{x}_R(t), \alpha_m, \beta_m) \{A_i(\alpha_m, \beta_m) \hat{x}_R(t) + B_i(\alpha_m, \beta_m) u_R(t) + L_i (y_R(t) - \hat{y}_R(t))\}}{\sum_{i=1}^r w_i(\hat{x}_R(t), \alpha_m, \beta_m)}, \tag{15}$$

$$\text{where } 0 \leq \alpha_j(t) \leq 1, \quad \sum_{j=1}^n \alpha_j(t) = 1. \quad (16)$$

The closed-loop machine learning fuzzy relaxed system is rewritten as follows:

$$\dot{x}_R(t) = \frac{\sum_{i=1}^r \sum_{j=1}^r w_i(\hat{x}_R(t), \alpha_m, \beta_m) w_j(\hat{x}_R(t), \alpha_m, \beta_m) \{A_i(\alpha_m, \beta_m)x_R(t) - B_i(\alpha_m, \beta_m)K_j\hat{x}_R(t)\}}{\sum_{i=1}^r \sum_{j=1}^r w_i(\hat{x}_R(t), \alpha_m, \beta_m) w_j(\hat{x}_R(t), \alpha_m, \beta_m)}, \quad (17)$$

$$\dot{\hat{x}}_R(t) = \frac{\sum_{i=1}^r \sum_{j=1}^r w_i(x_R(t), \alpha_m, \beta_m) w_j(\hat{x}_R(t), \alpha_m, \beta_m) \{(A_i(\alpha_m, \beta_m) - B_i(\alpha_m, \beta_m)K_j)\hat{x}_R(t) + L_i D_j(\alpha_m, \beta_m)(x_R(t) - \hat{x}_R(t))\}}{\sum_{i=1}^r \sum_{j=1}^r w_i(x_R(t), \alpha_m, \beta_m) w_j(\hat{x}_R(t), \alpha_m, \beta_m)}. \quad (18)$$

Therefore, the augmented systems can be represented as follows:

$$\dot{x}_{Ra}(t) = \frac{\sum_{i=1}^r \sum_{j=1}^r \sum_{s=1}^r w_i(x_R(t), \alpha_m, \beta_m) w_j(\hat{x}_R(t), \alpha_m, \beta_m) w_s(\hat{x}_R(t), \alpha_m, \beta_m) \tilde{A}_{ijs} x_{Ra}(t)}{\sum_{i=1}^r \sum_{j=1}^r \sum_{s=1}^r w_i(x_R(t), \alpha_m, \beta_m) w_j(\hat{x}_R(t), \alpha_m, \beta_m) w_s(\hat{x}_R(t), \alpha_m, \beta_m)}, \quad (19)$$

where

$$x_{Ra}(t) = \begin{bmatrix} x_R(t) \\ \tilde{x}_R(t) \end{bmatrix}, \quad \tilde{A}_{ijs}(\alpha_m, \beta_m) = \begin{bmatrix} A_i(\alpha_m, \beta_m) - B_i(\alpha_m, \beta_m)K_s & B_i(\alpha_m, \beta_m)K_s \\ S_{ijs}^1(\alpha_m, \beta_m) & S_{ijs}^2(\alpha_m, \beta_m) \end{bmatrix},$$

$$S_{ijs}^1(\alpha_m, \beta_m) = (A_i(\alpha_m, \beta_m) - A_j(\alpha_m, \beta_m)) - (B_i(\alpha_m, \beta_m) - B_j(\alpha_m, \beta_m))K_s + L_j(D_s(\alpha_m, \beta_m) - D_i(\alpha_m, \beta_m)),$$

$$\text{and } S_{ijs}^2(\alpha_m, \beta_m) = A_j(\alpha_m, \beta_m) - L_j D_s(\alpha_m, \beta_m) - (B_i(\alpha_m, \beta_m) - B_j(\alpha_m, \beta_m))K_s.$$

3. Neural Network Model for Chaotic Systems. From the discussion above, we can infer that if the dither has a sufficiently large frequency and a proper membership function in fuzzy relaxed system and dithered chaotic system is suitably chosen. This enables a rigorous prediction of the stability of the closed-loop dithered chaotic system by establishing that of the closed-loop machine learning fuzzy relaxed system.

A neural-network-based model is described as follows:

$$\dot{X}(t) = \Psi^S (W^S \Psi^{S-1} (W^{S-1} \Psi^{S-2} (\dots \Psi^2 (W^2 \Psi^1 (W^1 \Lambda(t))) \dots))), \quad (20)$$

where $\Lambda^T(t) = [X^T(t) \quad U^T(t)]$, with $X^T(t) = [x_1(t) \quad x_2(t) \quad \dots \quad x_\delta(t)]$. We assume S layers and each layer has R^σ ($\sigma = 1, 2, \dots, S$) neurons, in which $x_1(t) \sim x_\delta(t)$ and $u_1(t) \sim u_m(t)$ are the input variables. The notation W^σ denotes the weight matrix of the σ th ($\sigma = 1, 2, \dots, S$) layer. The transfer function vector of the σ th layer is defined as $\Psi^\sigma(v) \equiv [T(v_1) \quad T(v_2) \quad \dots \quad T(v_{R^\sigma})]^T$.

The Neural Network Differential Inclusion (NNDI) system can be described in the state-space representation (see Hu [23] and Liu et al. [24]) as follows:

$$\dot{Y}(t) = A(a(t))Y(t), \quad A(a(t)) = \sum_{i=1}^r h_i(a(t))\bar{A}_i, \quad (21)$$

According to the interpolation method and Equation (19), we can obtain:

$$\begin{aligned} \dot{X}(t) &= \left[\sum_{\zeta^S=1}^2 h_{\zeta^S}(t) G_{\zeta^S}^S \left(W^S \left[\dots \left[\sum_{\zeta^2=1}^2 h_{\zeta^2}(t) G_{\zeta^2}^2 \left(W^2 \left[\sum_{\zeta^1=1}^2 h_{\zeta^1}(t) G_{\zeta^1}^1 (W^1 \Lambda(t)) \right] \right) \right] \dots \right) \right] \right] \\ &= \sum_{\Omega^\sigma} h_{\Omega^\sigma}(t) E_{\Omega^\sigma} \Lambda(t). \end{aligned} \quad (22)$$

Finally, based on Equation (22), the dynamics of the NN model (18) can be rewritten as the following Neural Network Differential Inclusion (NNDI) state-space representation:

$$\dot{X}(t) = \sum_{i=1}^r h_i(t) \bar{E}_i \Lambda(t). \tag{23}$$

The NNDI state-space representation (23) can be further rearranged as follows:

$$\dot{X}(t) = \sum_{i=1}^r h_i(t) \{A_i X(t)\}, \tag{24}$$

where A_i is the partitions of E_i corresponding to the partition $\Lambda(t)$.

Based on the above modeling schemes for the NN-based approach, the nonlinear structural system can be approximated as an NNDI representation (24). The NNDI representation follows the same rules as the T-S machine learning fuzzy model, which combines the flexibility of machine learning fuzzy logic theory and the rigorous mathematical analysis tools of a linear system theory into a unified framework. To ensure the stability of the TLP system, the T-S machine learning fuzzy model and the stability analysis are recalled. First, the i th rule of the T-S machine learning fuzzy model, representing the structural system, can be represented as follows:

Rule i : IF $x_1(t)$ is M_{i1} and \dots and $x_p(t)$ is M_{ip} ,

THEN $\dot{X}(t) = A_i X(t) + \bar{A}_i X(t - \tau) + E_i \phi(t), \tag{25}$

where $i = 1, 2, \dots, r$ and r is the rule number; $X(t)$ is the state vector; M_{ip} ($p = 1, 2, \dots, g$) are the machine learning fuzzy sets and $x_1(t) \sim x_p(t)$ are the premise variables. Through using the machine learning fuzzy inference method with a singleton fuzzifier, product inference, and center average defuzzifier, the dynamic machine learning fuzzy model (25) can be expressed as follows [16,17]:

$$\dot{X}(t) = \frac{\sum_{i=1}^r w_i(t) [A_i X(t) + \bar{A}_i X(t - \tau) + E_i \phi(t)]}{\sum_{i=1}^r w_i(t)} = \sum_{i=1}^r h_i(t) [A_i X(t) + \bar{A}_i X(t - \tau) + E_i \phi(t)].$$

4. Example. In order to verify the feasibility of our approach in a practical physical system, a modified Chua’s circuit system is considered as follows [3]:

$$\begin{cases} \dot{x}_1 = p(x_2 - f(x_1)) = p \left(x_2 - \frac{1}{7}(2x_1^3 - x_1) \right) \\ \dot{x}_2 = x_1 - x_2 + x_3 \\ \dot{x}_3 = -qx_2 \end{cases} \tag{26}$$

where $p > 0$ and $q > 0$ are system parameters; x_1 and x_2 are the voltages across two capacitors; and x_3 is the current through the inductor. According to the tests in [3], the system parameters ($p = 10$, $q = 100/7$, and the initial condition 0.65) would make the uncontrolled modified Chua’s circuit (26) exhibit a chaotic attractor (as shown in Figure 2); specifically the so-called double scroll attractor. Therefore, a dither $d(t)$ with sufficiently high frequency is added in front of the nonlinearity $f(\cdot)$ to eliminate the chaotic motion. Hence, the modified Chua’s circuit with dither can be written as follows:

$$\dot{x}_1(t) = 10(x_2(t) - f(x_1(t) + d(t))); \dot{x}_2(t) = x_1(t) - x_2(t) + x_3(t); \dot{x}_3(t) = -\frac{100}{7}x_2(t) \tag{27}$$

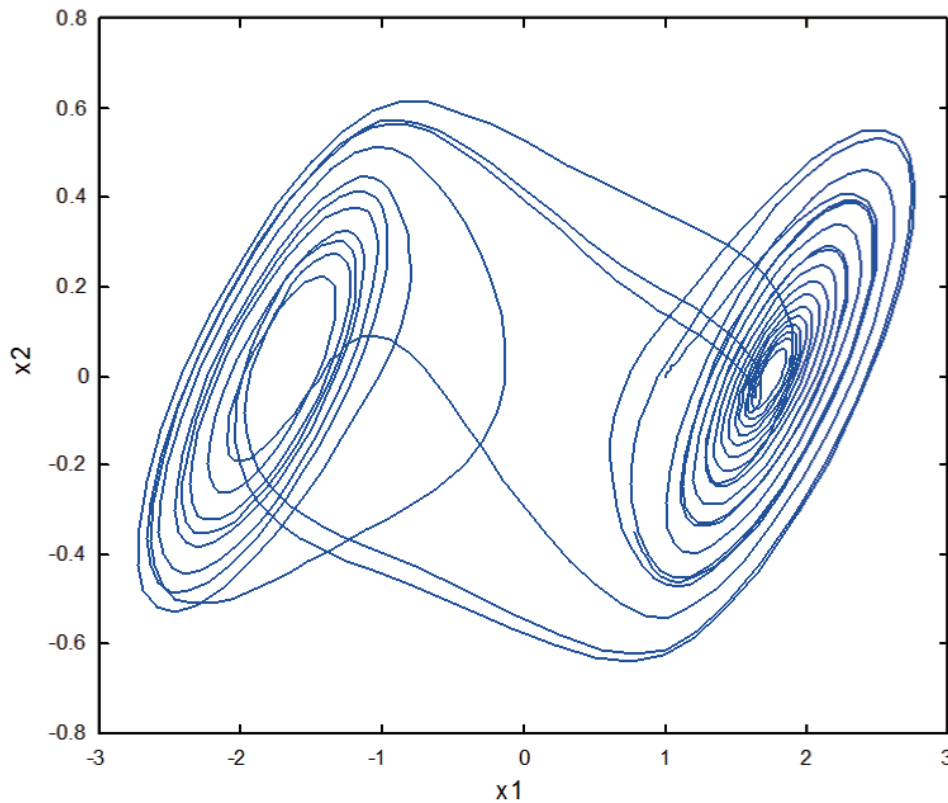


FIGURE 2. Phase portrait of the Chua's circuit

We try to find a dither signal for the modified Chua's circuit in the form of a square-wave. Based on (3), the corresponding relaxed model of the dithered Chua's circuit (27) is established as the following equations:

$$\begin{aligned} \dot{x}_{1r}(t) &= 10(x_{2r}(t) - \alpha_1(t)f(x_{1r}(t) + \beta_1(t)) - \alpha_2(t)f(x_{1r}(t) + \beta_2(t))); \\ \dot{x}_{2r}(t) &= x_{1r}(t) - x_{2r}(t) + x_{3r}(t); \quad \dot{x}_{3r}(t) = -\frac{100}{7}x_{2r}(t) \end{aligned} \quad (28)$$

in which

$$\alpha_2(t) = 1 - \alpha_1(t), \quad (29)$$

$$\alpha_1(t) = 0.5, \quad \alpha_2(t) = 0.5, \quad (30)$$

$$\beta_1(t) = -\beta_2(t) = A, \quad (31)$$

where A is a real constant number. Substituting (30) and (31) into (28), we have

$$\begin{aligned} \dot{x}_{1r}(t) &= 10 \left(x_{2r}(t) - \frac{1}{7} (2x_{1r}^3(t) + 6A^2x_{1r}(t) - x_{1r}(t)) \right); \\ \dot{x}_{2r}(t) &= x_{1r}(t) - x_{2r}(t) + x_{3r}(t); \quad \dot{x}_{3r}(t) = -\frac{100}{7}x_{2r}(t). \end{aligned} \quad (32)$$

Every temporary state of the inverted pendulum system can be decomposed by fuzzy IF-THEN rules; by combining all decomposed fuzzy IF-THEN rules, the whole nonlinear system can be approximated. Similar schemes can be found in previous studies. Hence, the approximated nonlinear system via T-S fuzzy model is decomposed as follows:

Rule 1: IF $x \geq \frac{\pi}{3}$, THEN $\dot{x} = \mathbf{A}_1\tilde{x} + \mathbf{B}_1u$; Rule 2: IF $x \approx \frac{\pi}{90}$, THEN $\dot{x} = \mathbf{A}_2\tilde{x} + \mathbf{B}_2u$.

We approximate the nonlinear function $g(v_{C_1})$ by a fuzzy model. A fuzzy approximation method, proposed by [14,15], is used to approximate the nonlinear function. The nonlinear

function can be exactly described by a fuzzy model,

$$g_1(v_{C_1}) \leq g(v_{C_1}) \leq g_2(v_{C_1}).$$

By means of Laypunov's direct method, one can get that the relaxed system (32) is asymptotically stable if A (the amplitude of dither) is greater than 1.65. Here, we let the frequency of the symmetrical square-wave dither be 2000 rad/s and plot the bifurcation diagram (maxima of $x_1(t)$ versus A) of the dithered Chua's circuit (27) in Figure 3. It shows that the dither with amplitude greater than 1.65 can convert the chaotic motion into a steady state. When the symmetrical square-wave dither with $A = 1.7$ is added after 60 seconds, the time responses of $x_1(t)$ for the relaxed system (11) and the modified Chua's circuit with dither ($\omega = 200$ rad/s and $\omega = 2000$ rad/s) are shown in Figure 4.

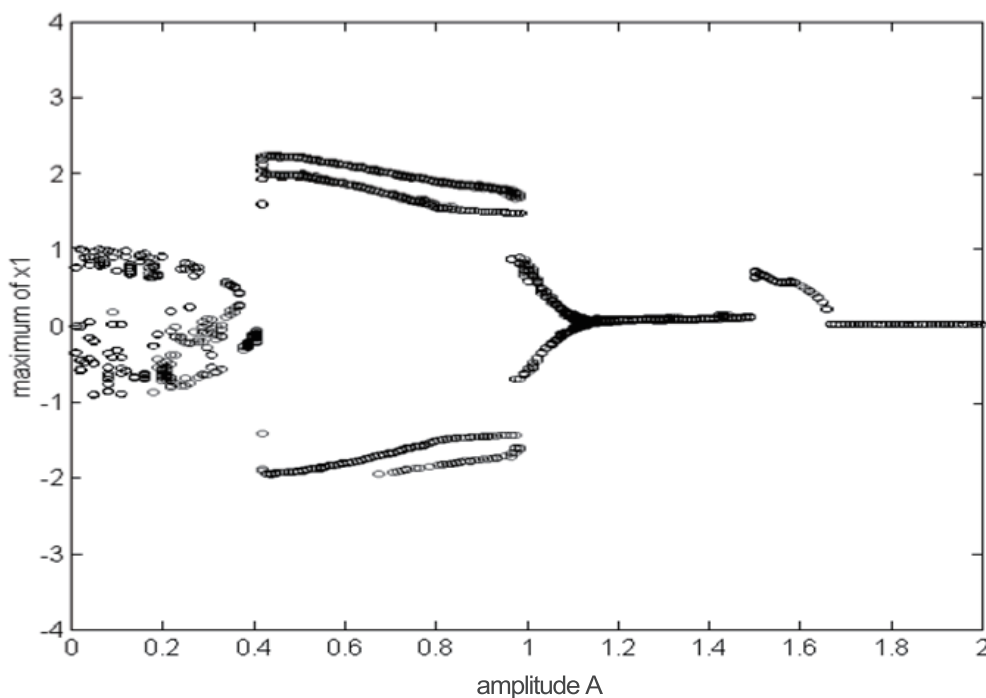
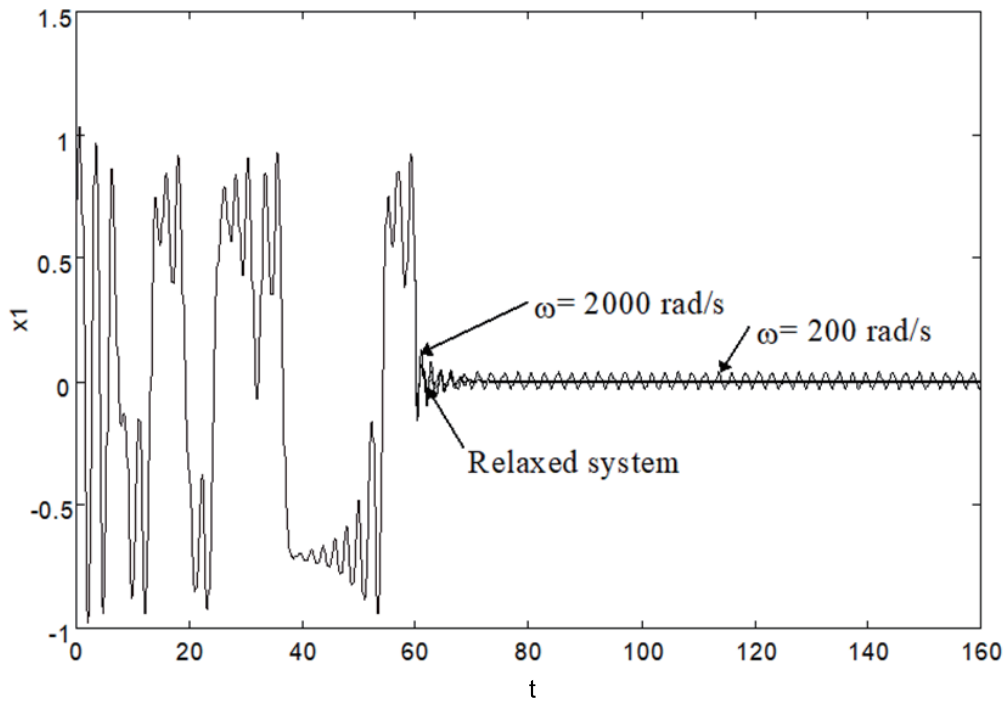
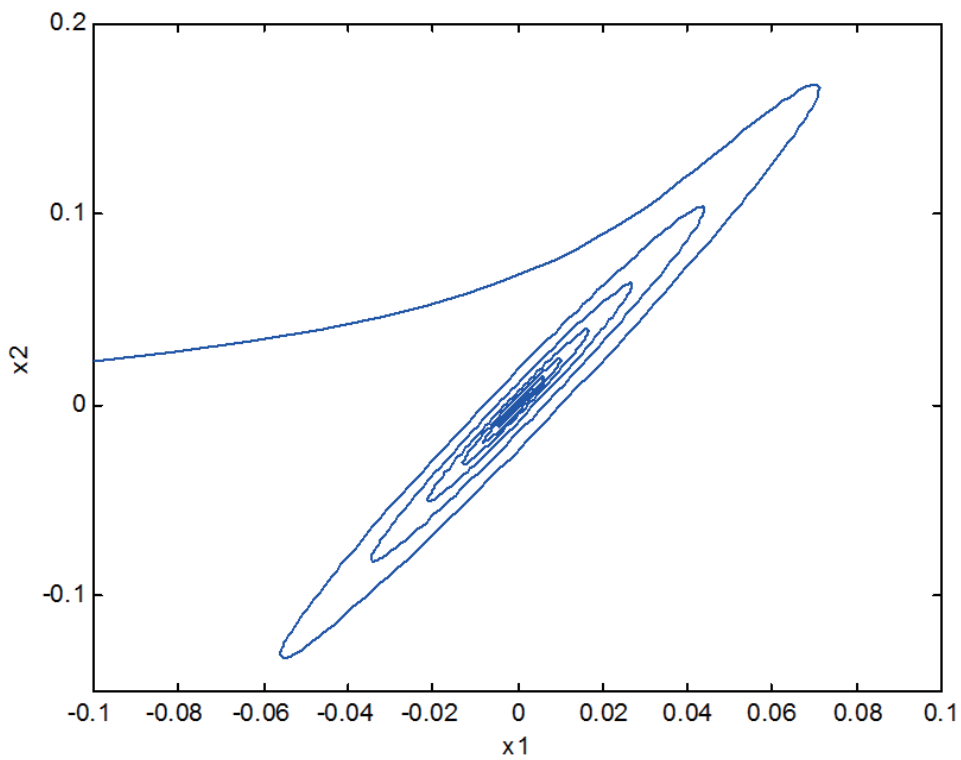


FIGURE 3. Bifurcation diagram with a symmetrical square-wave

We can see from Figure 4 that the system converges to a steady state after injecting the dither signal. The phase portrait of the relaxed system (11) with $A = 1.7$ is shown in Figure 5. Moreover, Figure 6 and Figure 7 are the phase portraits of the modified Chua's circuit with a symmetrical square-wave dither ($A = 1.7$, $\omega = 2000$ rad/s) and a symmetrical square-wave dither ($A = 1.7$, $\omega = 200$ rad/s), respectively. It is obvious that the trajectory of the dithered Chua's circuit system is approximated by the trajectory of its corresponding relaxed system and the approximation improves as the frequency of dither increases. This fact enables us to get a rigorous prediction of the dithered chaotic system's behavior by establishing that of the relaxed system. The results should be generally applicable to other chaotic systems as the principle is the same.

5. Conclusions. A novel fuzzy controller for chaotic systems is proposed in this paper. If a fuzzy controller cannot stabilize the chaotic system, a dither, as an auxiliary of the controller, is injected into the chaotic system and then the chaotic system is stabilized asymptotically by regulating the dither's parameters. In this study, a fuzzy controller and a fuzzy observer are proposed via the parallel distributed compensation technique to stabilize the chaotic system.

FIGURE 4. Time responses of the state x_1 FIGURE 5. Phase portrait of the relaxed system with $A = 1.7$

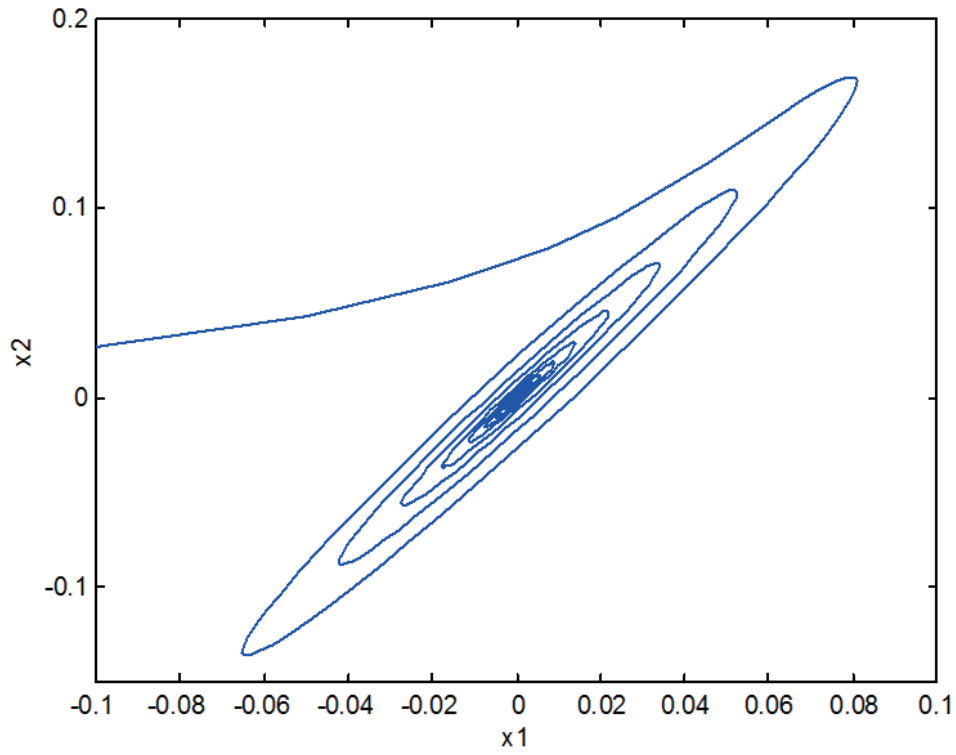


FIGURE 6. Phase portrait Chua's circuit dither (2000 rad/s)

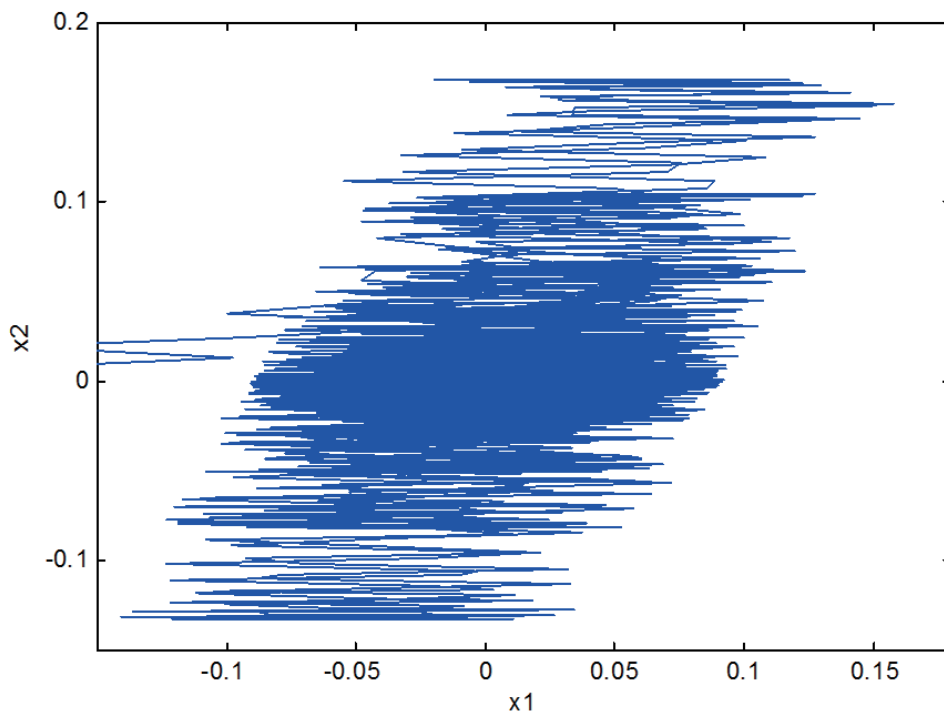


FIGURE 7. Phase portrait with a symmetrical square-wave dither

Acknowledgment. The authors declare that there are no conflicts of interest regarding the publication of this paper.

REFERENCES

- [1] J. Singer, Y.-Z. Wang and H. H. Bau, Controlling a chaotic system, *Phys. Rev. Lett.*, vol.66, no.9, pp.1123-1125, 1991.
- [2] T. Kapitaniak, L. J. Kocarev and L. O. Chua, Controlling chaos without feedback and control signals, *Int. J. Bifurcation Chaos*, vol.3, p.459, 1993.
- [3] C.-C. Hwang, H.-Y. Chow and Y.-K. Wang, A new feedback control of a modified Chua's circuit system, *Physica D*, vol.92, pp.95-100, 1996.
- [4] H. O. Wang and E. H. Abed, Bifurcation control of a chaotic system, *Automatica*, vol.31, p.1213, 1995.
- [5] A. Azevedo and S. M. Rezende, Controlling chaos in spin-wave instabilities, *Phys. Rev. Lett.*, vol.66, pp.1342-1345, 1991.
- [6] D. J. Gauthier et al., Stabilizing unstable periodic orbits in a fast diode resonator using continuous time-delay autosynchronization, *Phys. Rev. E*, vol.50, no.3, pp.2343-2346, 1994.
- [7] P. Colet and Y. Braiman, Control of chaos in multimode solid state lasers by the use of small periodic perturbations, *Phys. Rev. E*, vol.53, pp.200-206, 1995.
- [8] E. Ott, C. Grebogi and J. A. Yorke, Controlling chaos, *Phys. Rev. Lett.*, vol.64, no.11, pp.1196-1199, 1990.
- [9] A.-R. José, Nonlinear feedback for controlling the Lorenz equation, *Phys. Rev. E*, vol.50, no.3, pp.2339-2342, 1994.
- [10] C. A. Desoer and S. M. Shahruz, Stability of the dithered nonlinear system with backlash or hysteresis, *Int. J. Control*, vol.43, no.4, pp.1045-1060, 1986.
- [11] A. M. Steinberg and I. Kadushin, Stabilization of nonlinear systems with a dither control, *J. Math. Anal. Appl.*, vol.43, pp.273-284, 1973.
- [12] J. Warga, Relaxed variational problem, *J. Math. Anal. Appl.*, vol.4, pp.111-128, 1962.
- [13] A. J. McDaid and B. R. Mace, A robust adaptive tuned vibration absorber using semi-passive shunt electronics, *IEEE Trans. Ind. Electron.*, vol.63, pp.5069-5077, 2016.
- [14] J. Nečásek, J. Václavík and P. Marton, Digital synthetic impedance for application in vibration damping, *Rev. Sci. Instrum.*, vol.87, no.2, p.024704, 2016.
- [15] J. Pérez-Díaz, I. Valiente-Blanco and C. Cristache, Z-damper: A new paradigm for attenuation of vibrations, *Machines*, vol.4, pp.1-11, 2016.
- [16] W. Shen, S. Zhu, H. Zhu and Y.-L. Xu, Electromagnetic energy harvesting from structural vibrations during earthquakes, *Smart Struct. Syst.*, vol.18, no.3, pp.449-470, 2016.
- [17] B. Yan et al., Self-powered electromagnetic energy harvesting for the low power consumption electronics: Design and experiment, *Int. J. Appl. Electromagn. Mech.*, vol.54, pp.1-11, 2017.
- [18] F. Kang, J. Li and J. Li, System reliability analysis of slopes using least squares support vector machines with particle swarm optimization, *Neurocomputing*, vol.209, pp.46-56, 2016.
- [19] F. Khademi, S. M. Jamal, N. Deshpande et al., Predicting strength of recycled aggregate concrete using artificial neural network, adaptive neuro-fuzzy inference system and multiple linear regression, *Int. J. Sustainable Built Environment*, vol.5, pp.355-369, 2016.
- [20] M. Kandi-D, M. Soleymani and A. A. Ghadimi, Designing an optimal fuzzy controller for a fuel cell vehicle considering driving patterns, *Scientia Iranica*, vol.23, pp.218-227, 2016.
- [21] M. Khanzadi et al., An integrated fuzzy multi-criteria group decision making approach for project delivery system selection, *Scientia Iranica*, vol.23, pp.802-814, 2016.
- [22] A. Mahmoudi, S. Sadi-Nezhad and A. Makui, An extended fuzzy VIKOR for group decision-making based on fuzzy distance to supplier selection, *Scientia Iranica*, vol.23, pp.1879-1892, 2016.
- [23] Y.-C. Hu, Incorporating a non-additive decision making method into multi-layer neural networks and its application to financial distress analysis, *Knowledge-Based Systems*, vol.21, no.5, pp.383-390, 2008.
- [24] Y.-J. Liu, S. Tong and Y. Li, Adaptive neural network tracking control for a class of non-linear systems, *International Journal of Systems Science*, vol.41, no.2, pp.143-158, 2010.